Analytical Methods

Accepted Manuscript

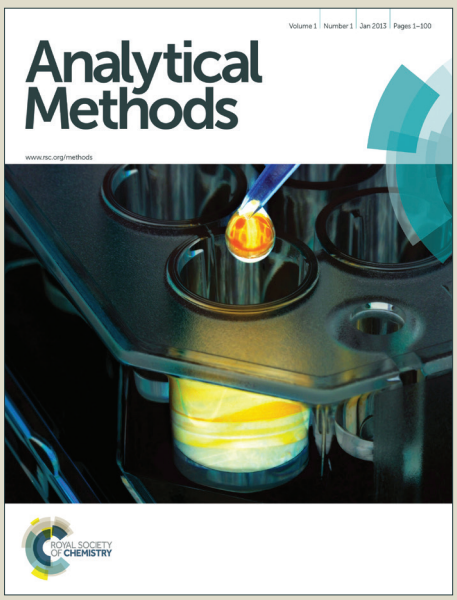

ROYAL SOCIETY OF CHEMISTRY

www.rsc.org/methods

Journal Name

RSCPublishing

Article

A novel *rhodamine-3,4-dihydro-2H-1,3-benzoxazine* conjugate as a highly sensitive and selective chemosensor for Fe^{3+} ion with cytoplasmic cell imaging possibilities

Habib Ali Molla[a], Rahul Bhowmick[a], Atul Katarkar[b], Keya Chaudhuri[b], Sumana Gangopadhyay[c], and Mahammad Ali[a,*]

Cite this: DOI: 10.1039/x0xx00000x

Received 00th February 2015,
Accepted 00th XXXX 2015

DOI: 10.1039/x0xx00000x

www.rsc.org/

A novel, highly sensitive and selective fluorescent chemosensor '*rhodamine-3,4-Dihydro-2H-1,3-benzo-xazine*' [RH-BZN (1)] has been synthesized and characterized by single crystal X-ray diffraction and other physicochemical techniques. In 3:7 water:MeCN (v/v) at pH 7.2 (10 mM HEPES buffer, μ = 0.05 M LiCl) it selectively recognizes Fe^{3+} through 1:1 complex formation resulting a 240 fold fluorescence enhancement and a binding constant (K_f) of 1.50 x 10^4 M^{-1}. The otherwise non-fluorescent spirolactum form of the probe results a dual changes in absorbance and fluorescence arising out of opening of the spirolactum ring through coordination to Fe^{3+} ion. This probe could suitably be employed for cytoplasmic intracellular imaging of Fe^{3+} without notable cytotoxicity. The reversible binding RH-BZN to Fe^{3+} was confirmed by reacting with tetra-*n*-butylammonium fluoride both in extra- and intra-cellular conditions.

Transition-metal ions involve in many biological and environmental processes, and a great emergence of interest has developed in recent years to generate metal ion selective and sensitive fluorescent probes.[1] Though numerous excellent works focusing on the selective and sensitive detection of transition metal ions; e.g., Cu^{2+}, Pb^{2+}, Zn^{2+}, and Hg^{2+} have been reported[2], examples of Fe^{3+}-selective fluorescent probes are still scarce[3]; despite the indispensable role of Fe^{3+} in many biochemical processes.[4,5]

Iron seems to be a versatile element involved in the proper functioning of numerous biological systems in all living organisms including bacteria and plants.[6,7] Both deficiency and excess of iron can induce a variety of diseases.[8] Iron being both useful and cytotoxic,[9] its deficiency throughout the developmental phases may lead to permanent loss of motor skills.[10] Iron overload in a living cell can lead to generation of reactive oxygen species (ROS) via the Fenton reaction, which can cause damage to lipids, nucleic acids, and proteins. Again, accumulation of iron in the central nervous system may lead to a number of diseases like Parkinson, Huntington and Alzheimers.[9a]Keeping in view of the roles played by iron in day-to-day life, the development of techniques for selective determination of iron is in great demand. It is necessary to design simple, highly sensitive and selective chemosensor for Fe^{3+} detection and establish a method for the determination of trace amounts of Fe^{3+} ions. Most of the known Fe^{3+} sensors are based on fluorescence quenching mechanisms due to the paramagnetic nature of ferric ions.[11] In addition, most turn-on fluorescence sensors for Fe^{3+} are not selective over Cr^{3+} and Cu^{2+}.[12] Therefore, the development of a chemosensor that shows high selectivity for iron involving a fluorescence turn-on response is necessary for practical applications.

On the other hand, *3,4-Dihydro-2H-1,3-benzoxazine*s are bicyclic heterocycles that are of significant interest in the polymeric and pharmacological fields. 1,3-Benzoxazines have long been recognized for their wide range biological activities with uses as herbicides and agricultural microbiocides, bactericide, fungicide, antidepressive, anti-inflammatory, and antitumor agents.[13-16] Moreover, 1,3-benzoxazine monomers are recently used to develop a new type of phenolic resin, namely polybenzoxazines, by the ring-opening polymerization.[17-20]

Rhodamine based conjugate with spirolactam structure are, in general, non-fluorescent but acts as colorimetric as well as fluorometric sensors with the enhancement of absorption and fluorescence emission intensity, respectively on selective binding to metal ion(s).

In the present communication, we are going to disclose, for the first time, a *Rhodamine-3,4-Dihydro-2H-1,3-benzoxazine* conjugate as a highly sensitive and selective fluorescent chemosensor for Fe^{3+} ion which further recognizes F^- ion by quenching the fluorescence of Fe^{3+}-**RH-BZN** complex by abstracting the metal ion through the formation of stable FeF_6^{3-} complex.

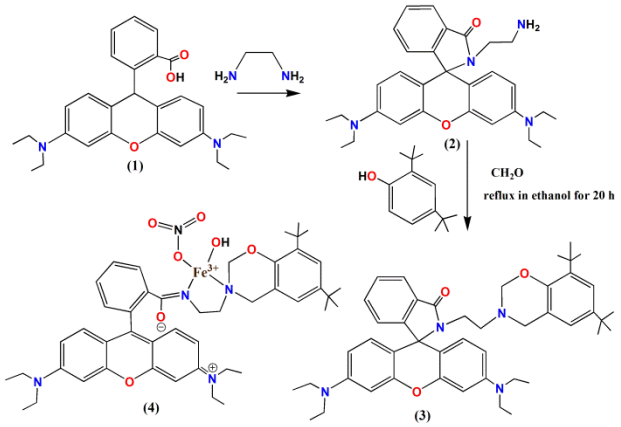

Scheme-1

Experimental

Materials and Methods.

The starting materials, such as, rhodamine B hydrochloride (Sigma Aldrich), 2,4-di-*tert*-butyl phenol (Sigma Aldrich), ethylene diamine (Sigma Aldrich), formaldehyde (Sigma Aldrich) and ferric nitrate (Sigma Aldrich), tetra-*n*-butylammonium fluoride (Sigma Aldrich) were used for the preparation of RH-BZN and Fe^{3+} complex. Other metal ions were obtained from the previous studies. Solvents like EtOH, MeOH, MeCN etc (Merck, India) were of HPLC grade. MeCN and deionised water were used for spectroscopic studies.

Physical Measurements

Infrared spectra (400–4000 cm^{-1}) were recorded from KBr pellets on Nickolet Magna IR 750 series-II FTIR spectrophotometer. ^{1}H-NMR and ^{13}C-NMR was recorded in $CDCl_3$ on a Bruker 300 MHz NMR spectrometer using tetramethylsilane (δ = 0) as an internal standard. UV-Vis spectra were recorded on Agilent diode-array spectrophotometer (Model, Agilent 8453), Steady-state Fluorescence spectra were recorded on a PTI spectrofluorimeter (Model QM-40.), ESI-MS^+ (m/z) of the RH-BZN and Fe^{3+} complex were recorded on a HRMS spectrometer (Model: XeVO G2 QTof).

Syntheses

Preparation of RH-BZN

Rhodamine B hydrochloride (**1**) (5.0 mmol) and ethylenediamine (10.0 mmol) were dissolved in EtOH and refluxed for 6 hours with continuous stirring whereupon a white crystalline solid of rhodamine-amine (**2**) was deposited. The solid was filtered and washed with EtOH. The compound (**2**) (2 mmol), 2,4-di tertiary butyl phenol (4 mmol) and formaldehyde (4 mmol) were dissolved in MeCN and refluxed for 20 h with constant stirring whereupon a white solid deposited was filtered and washed several times with ethanol and dried in air (68 % yield). It was further recrystallized from MeOH to get single crystals suitable for X-ray diffraction studies. ^{1}H NMR (300 MHz, $CDCl_3$) (δ, ppm): 1.20(t, 12H, CH_3) , 1.28(t, 18H, CH_3), 2.48(s, 2H, CH_2), 3.36(s, 8H, CH_2), 3.83(s, 2H, CH_2), 4.60(s, 2H, CH_2), 6.28(s, 2H, CH_2), 6.40-6.50(m, 4H, ArH), 6.73(1H,s, ArH), 7.09(s,2H, ArH), 7.29(s, 1H, ArH), 7.46(s, 2H, ArH), 7. 92(s, 1H, ArH) (**Fig. S1-S2**). IR spectrum: ṽ = 1692.15 cm^{-1} (spirolactam amide-keto), 1615.02 cm^{-1} (–C=N) (**Fig. S3**). ESI-MS^+ (m/z):715.37 (RH-BZN + H^+) (**Fig. S4**).

Synthesis of [Fe (**RH-BZN**)$(NO_3)_2(CH_3CN)$]]

Fe $(NO_3)_3.9H_2O$ (2 mmol) in 5 ml MeCN was added drop wisely to a solution of **RH-BZN** (2 mmol) in 20 ml MeCN with continuous stirring. After 1 hour the solution was filtered and kept aside undisturbed. After one day crystalline complex was precipitated out. It was collected by filtration, washed several times with MeOH and dried in air. It was recrystallized from methanol. Several trials to grow single crystals were failed. IR spectrum: ṽ = 1637.68 cm^{-1} (spirolactam amide-keto), 1554.65 cm^{-1} (–C=N) (**Fig. S3**). ESI-MS^+ (m/z): 834.4961 [Fe(**RH- BZN**)$(OCH_3)(CH_3OH)$];934.5900 [Fe(**RH-BZN**)$(NO_3)_2(CH_3CN)$]; 948.6159 [Fe(**RHBZN**)$(NO_3)_2(OCH_3)$]Na^+ (**Fig. S5**).

Cell culture

Human hepatocellular liver carcinoma (HepG2) cells line (NCCS, Pune, India), were grown in DMEM supplemented with 10% FBS and antibiotics (penicillin, 100 µg/ml; streptomycin, 50 µg/ml). Cells were cultured at 37 °C in 95% air, 5% CO_2 incubator.

Cell Cytotoxicity Assay

To determine % cell viability of **RH-BZN**, MTT assay was performed. HepG2 cells (1×10^5 cells/well) were cultured in a 96 well plate at 37 °C, and exposed to varying concentrations of **RH-BZN**, 1, 10, 20, 40, 60, 80 and 100 µM respectively for 12h. 20 µl of MTT solution [5 mg/ml 1X phosphate-buffered saline (PBS)] was added to each well of a 96-well culture plate and again incubated continuously at 37^0C for a period of 4 h. All media were removed from wells and 100 µl of DMSO was added to each well and absorbance was measured at 550 nm (E_{Max} Precision MicroPlate Reader, Molecular Devices, USA). All experiments were performed in triplicate and the relative cell viability (%) was expressed as a percentage relative to the untreated control cells (**Fig. S6).**

Cell Imaging Study

HepG2 Cells were culture and incubated in 35x10 mm culture dish over cover slip for 24h at 37°C. The cells were allowed to incubate with 10 µm **RH-BZN** prepared by dissolving it in a mixed solvent (DMSO: water = 1:9 (v/v) in the culture medium, allowed to incubate for 30 min at 37 °C. After incubation, cells were washed twice with 1X PBS and allowed to counterstained by DAPI (2-(4-Amidinophenyl)-6-indolecarbamidine dihydrochloride- 4',6-diamidino-2-phenyl-indole, used for nuclear staining, Sigma). Fluorescence images of HepG2 cells were taken by a fluorescence microscope (Leica DM3000, Germany) with an objective lens of 40X magnification. Fluorescence images of HepG2 cells were taken separately from another set of experiment where cells were pre-incubated with 10 µM Fe^{3+} for 30 min at 37^0C followed by washing twice with 1X PBS and subsequent incubation with 10 µM **RH-BZN** for 30 min at 37^0C. Similarly, in another set of experiment, cells were incubated sequentially with 10 µm Fe^{3+}, 10 µM **RH-BZN** and 100 µM F^- for 30 min at 37^0C with alternative washing with 1X PBS two times. The live cell on cover slip was allowed for fluorescence imaging, **RH-BZN** shows HepG2 intracellular cytoplasmic red fluorescence by forming complex with Fe^{3+} and DAPI, used as counter stain to localize the nucleus, shows blue color at nucleus. Moreover, the concentration dependent capture of Fe^{3+} was preformed similarly as per described above at 1, 10 and 20 µM for **RH-BZN**. Furthermore, to confirm the cytoplasmic capturing of Fe^{3+} and cytoplasmic localization of **RH-BZN** after forming complex with Fe^{3+}, cell imaging study was conducted by using DAPI as nuclear counter stain and LysoTracker Green DND-26 (invitrogen) for cytoplasm and, live cell imaging study was carried out as described above. Likely, **RH-BZN** showed HepG2 intracellular cytoplasmic red fluorescence by forming complex with Fe^{3+}, confirmed against nuclear and cytoplasmic tracker.

Solution preparation for UV-Vis and fluorescence studies:

For both UV-Vis and fluorescence titrations, a stock solution of 1.0×10^{-3} M of the probe **3** was prepared by dissolving it in 0.5 ml MeCN and finally the volume is made up to 10 ml by MeCN. Similarly, 10 ml 1.0×10^{-3} M stock solutions of Fe^{3+} and tetra-*n*-butyl ammonium fluoride were prepared separately in MeCN. 100 ml solution of 10 mM HEPES buffer was prepared and pH was adjusted to 7.24 by using HCl and NaOH as required. 2.5 ml of this buffer solution was pipette out into a cuvette to which 20 µM of the probe was added and Fe^{3+} ions were added incrementally starting from 0 to 25 µM in a regular interval of volume and UV-Vis and fluorescence spectra were recorded for each solution. Similar is the case for tetra-*n*-butyl ammonium fluoride titration. Path length used of the cells for absorption and emission studies was 1 cm. Fluorescence measurements were performed using 2 nm x 2 nm slit width.

Quantum Yield Determination:

Fluorescence quantum yields (**Φ**) were estimated by integrating the area under the fluorescence curves with the equation:

$$\Phi_{sample} = \frac{OD_{std}}{OD_{sample}} \times \frac{A_{sample}}{A_{std}} \times \Phi_{std}$$

where, A is the area under the fluorescence spectral curve and OD is optical density of the compound at the excitation wavelength. The standard used for the measurement of fluorescence quantum yield was rhodamine 6G $\Phi_{std} = 0.94$ in CH_3OH).

Results and Discussion

As depicted in **Scheme 1**, receptor **RH-BZN (3)** was synthesized from the reaction of rhodamine-B with ethylenediamine followed by Mannich reaction with 2,4-di-*tert*-butylphenol in presence of formaldehyde in EtOH in refluxing conditions for 20 h with 68% yield. The final product (**3**) was well characterized by ^{1}H NMR (**Fig. S1**), ^{13}C-NMR (**Fig.S2**), IR (**Fig.S3**), HRMS (**Fig.S4 and S5**) and single crystal X-ray diffraction method (**Fig. 1**). Detail of the method of data collection and refinement are listed in **Table 1**.

Table 1 - Crystal Data and Details of the Structure Determination

Formula	C46 H58 N4 O3
Formula Weight	714.96
Crystal System	Monoclinic
Space group	P21/c (No. 14)
a, b, c [Å]	17.313(3) 24.678(4) 9.5642(17)
α, β, γ [°]	90 105.015(390
V [Å^3]	3946.8(12)
Z	4
D(calc) [g/cm^3]	1.203
μ(MoK$_\alpha$) [/mm]	0.075
F(000)	1544
Crystal Size [mm]	0.05x0.18 x0.23
Temperature (K)	296
Radiation [Å] MoK$_\alpha$	0.71073
Θ Min-Max [°]	1.2, 27.6
Dataset	-22: 22 ; -32: 32 ; -12: 12
Tot., Uniq. Data, R(int)	32636, 9136, 0.094
Observed data [I > 2.0 σ(I)]	4317
N$_{ref}$, N$_{par}$	9136, 492
R, wR$_2$, S	0.0861, 0.2329, 1.02
Max. and Av. Shift/Error	0.02, 0.02
Min. and Max. Resd. Dens. [e/Ang^3]	-0.55, 0.86
w = 1/[\s^2^(Fo^2^)+(0.2000P)^2^], where P=(Fo^2^+2Fc^2^)/3	

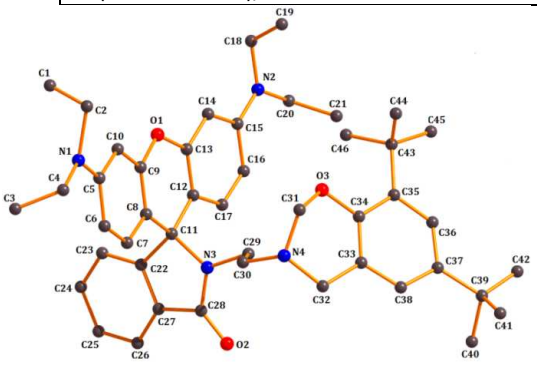

Fig. 1 Molecular view of **3**, H atoms are removed to get better clarity.

Single crystal X-ray diffraction studies reveal that the compound RH-BZN crystallises in monoclinic system of space group P21/c. The crystallographic details are depicted in Table 1.

The receptor **3** was found to be highly sensitive and selective colorimetric and fluorogenic dual sensor for Fe^{3+} while in the absence of Fe^{3+}; the solution of **3** is colourless and non-fluorescent.

In order to determine the stability constant and composition of the RH-BZN–Fe^{3+} complex we have carried out UV-Vis titration with fixed concentration of **3** (20 μM) with variable concentration of Fe^{3+} (0 - 35.0 μM) at 25 °C in aqueous MeCN (3:7, v/v, 1.0 mM HEPES buffer, pH 7.2, μ = 0.05 M LiCl). It was revealed that there is a gradual development of a new absorption band at around 552 nm on addition of Fe^{3+} (**Fig. 2a**). A plot absorbance vs. [Fe^{3+}] showed a gradual increase in absorbance and tends to become almost constant at ~1:1.75 ligand:metal mole ratio. The absorption titration data were fitted to a non-linear eqn. (1),[21] where *a* and *b* are the absorbance/fluorescence intensities in the absence and presence of excess metal ions, respectively, *c* (= K_f) is the formation constant and *n* is the stoichiometry of the reaction.

$$y = \frac{a + b*c*x^n}{1 + c*x^n} \qquad (1)$$

The evaluated parameters are: K_f = (1.50 ± 0.18) x 10^4 M^{-1}, *n* = 1.04 ± 0.01.

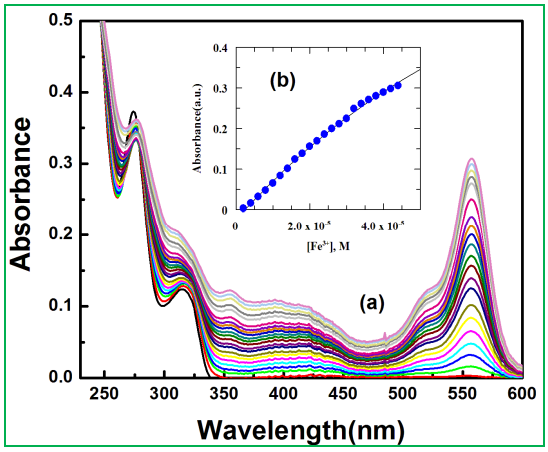

Fig. 2(a) Absorption titration of RH-BZN with Fe^{3+} in MeCN-H_2O (7:3, v/v) in HEPES buffer (1 mM) at pH 7.2; (b) non-linear fitting of data.

The fluorescence titration data were solved analogously as in case of absorption titration data which gives K_f of (1.50 ± 0.23) x 10^4 M^{-1}, n = 0.99 ± 0.02 (see **Fig. 3, B**). There is an excellent agreement between the K_f values extracted from absorption ($K_f = (1.50 \pm 0.18) \times 10^4\ M^{-1}$, $n = 1.04 \pm 0.01$) and fluorescence (K_f of (1.50 ± 0.23) x 10^4 M^{-1}, n = 0.99 ± 0.02) titration data manifesting the self-consistency of our results.

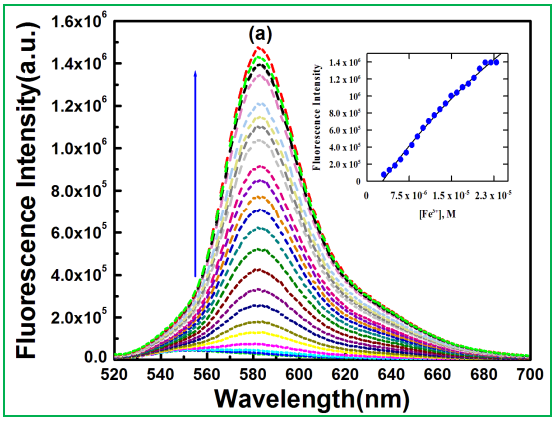

Fig. 3 (a) Fluorescence titration of (20.0 µM) in MeCN-H_2O (7:3, v/v) in HEPES buffer at pH 7.2 by the gradual addition Fe^{3+} withλ_{ex} = 510 nm, λ_{em} = 582 nm, Inset (b) non-linear curve-fit of F.I vs. [Fe^{3+}] plot.

After performing all possible composition of CH_3CN/H_2O for spectral (Fluorescence) studies it was observed that CH_3CN/H_2O (7:3, v/v) is a good choice for this study. On increasing the water content beyond CH_3CN/H_2O (7:3, v/v) the fluorescence enhancement was found to decrease progressively and there is no visible change in FI when 100% water was used (**Fig. S8**). The detection of Fe^{3+} was not perturbed by the presence of biologically abundant Na^+, K^+, Ca^{2+} and Mg^{2+} ions. Similarly, several transition-metal ions, namely Cr^{3+}, Mn^{2+}, Fe^{2+}, Co^{2+}, Cu^{2+}, Ni^{2+} and Zn^{2+}, and heavy-metal ions, like Cd^{2+}, Hg^{2+} and Pb^{2+} did not show any significant spectral change under identical reaction conditions and also carried out the selectivity studies both for individual metal ions as well as in presence of Fe^{3+} in each case. These studies clearly suggest that all the tested metal ions have no interference in the selective detection of Fe^{3+} (**Fig. S9**).

To check the suitability for the convenient biological application of this probe towards Fe^{3+} sensing under physiological conditions the pH-stability of the probe was investigated which showed no obvious fluorescence of **RH-BZN** between pH 6 and 12, suggesting the existence of spirolactum form of **RH-BZN** over this wide range of pH (**Fig. S10**). However, in presence of selective guest like Fe^{3+} ion it fluoresces effectively at pH ≥ 7.0 which clearly indicates the compatibility of the probe for biological applications under physiological conditions.

The reversible binding of **3** to Fe^{3+} was investigated in the same solvent system as was used in the absorption and fluorescence titrations. Anions like SO_4^{2-},NO_3^-,Cl^-, F^-, Br^-, I^-, OAc^- and N_3^- of 5 equivalents of **3** were introduced (**Fig. S11**) into the solution of **RH-BZN**–Fe^{3+} complex and subsequently the changes in their fluorescence intensities were monitored. The results showed that anion like F^- (tetra-*n*-butylammonium fluoride) have a strong affinity towards Fe^{3+} and their binding constants seems to be much higher than that of **RH-BZN**–Fe^{3+} complex resulting the abstraction of Fe^{3+} from the complex and bleaching of the emission band at 582 nm through the re-establishment of the spirolactum

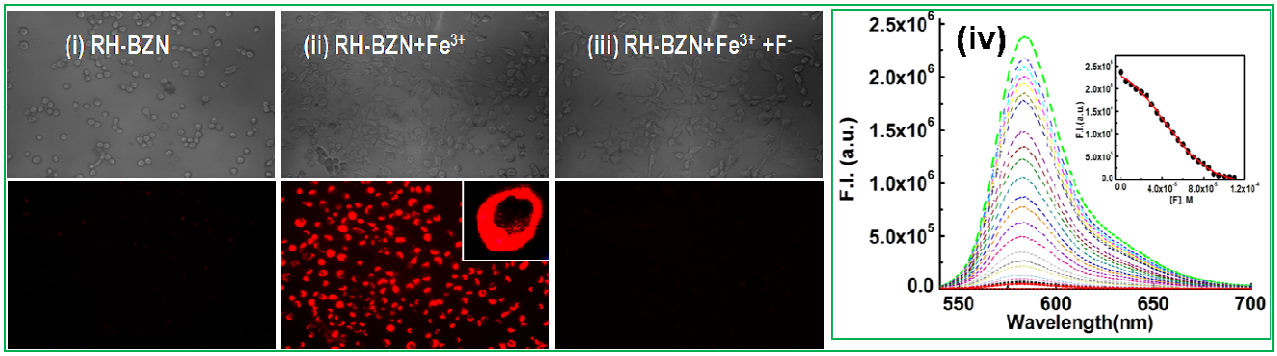

Fig. 4 The phase contrast (upper panel) and fluorescence images (lower panel) of HepG2 cells were captured (40X) after incubation with (i) **RH-BZN** (10 µM), (ii) **RH-BZN** + Fe^{3+} (10 µM each) and (iii) **RH-BZN** + Fe^{3+} (10 µM each) followed by addition of 100 µM F^- for 30 min at 37°C. Inset shows the cytoplasmic response of RH-BZN towards Fe^{3+}. (iv) Fluorescence titration of **RH-BZN**–Fe^{3+} ensemble (20 µM) by gradual addition of F^- solution (5 µM at a time).

Journal Name

RSCPublishing

Article

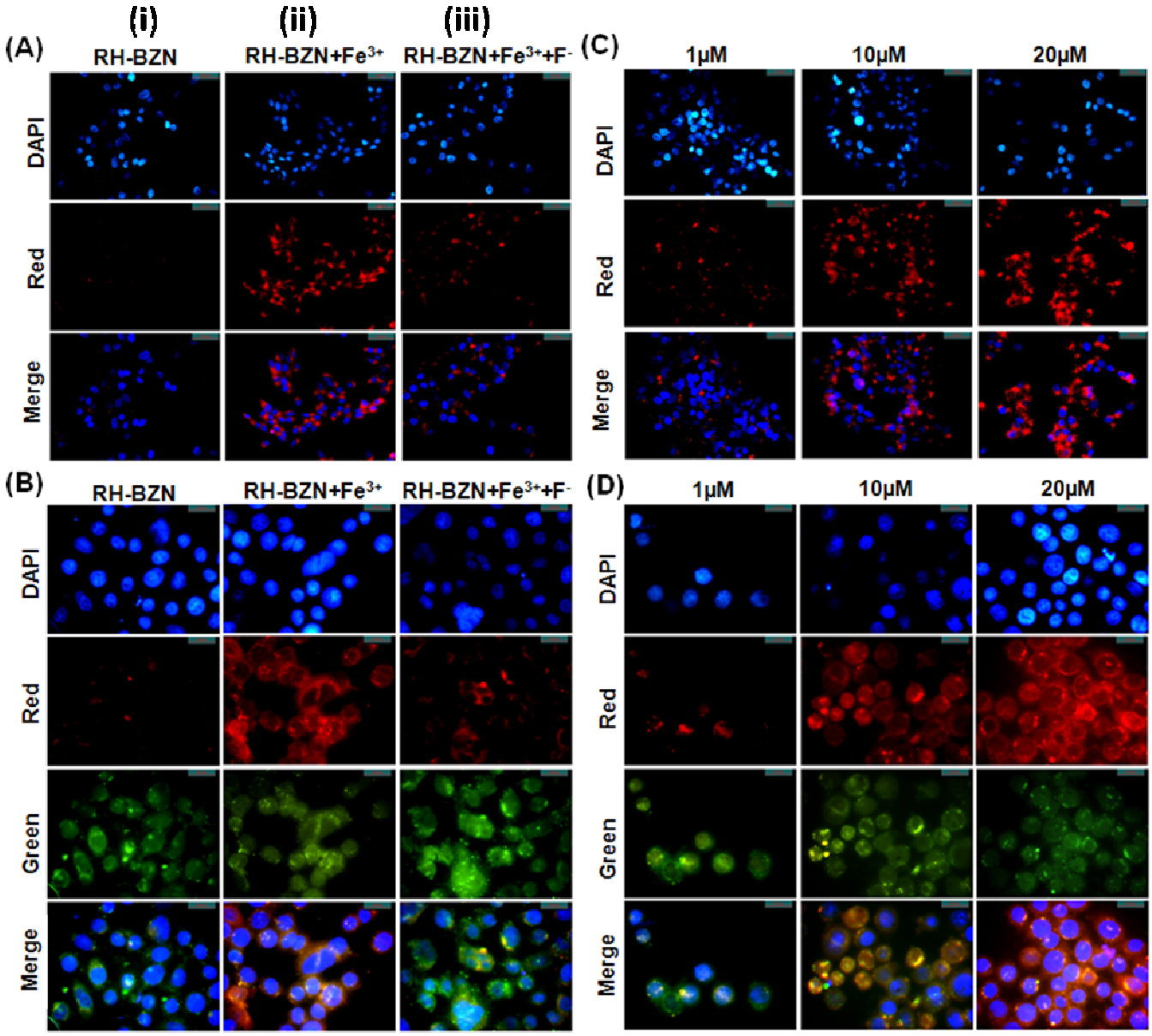

Fig. 5 HepG2 cells were incubated with (i) 10μM of **RH-BZN** for 30 min at 37 °C, (ii) pre-incubated 10μM of Fe^{3+} for 30 min at 37°C followed by washing twice with 1X PBS and, subsequent incubation with 10μM **RH-BZN** for 30 min at 37^0C and (iii) pre-incubated 10μM of Fe^{3+} for 30 min at 37°C followed by 10μM **RH-BZN** and 100μM F^- for 30 min at 37^0C with alternative washing with 1X PBS two times. **(A)** The fluorescence image (40X) shows the strong red florescence when **RH-BZN** complexes with Fe^{3+} (in green filter) and subsequently quench off on addition of F^- (in green filter). The merge image shows the cytoplasmic **RH-BZN** +Fe^{3+} fluorescence, suggests no nuclear entry of **RH-BZN** fluorophore, DAPI as nuclear counter stain (blue, in violet/blue filter). (**B**) The fluorescence image (100X) shows the strong red florescence when **RH-BZN** complexes with Fe^{3+} and subsequently quench off on addition of F^-. The merge image shows the cytoplasmic **RH-BZN** +Fe^{3+} fluorescence, suggests no nuclear entry of **RH-BZN** fluorophore, DAPI as nuclear counter stain (blue) and LysoTracker (Green, in blue filter) for cytoplasm. **(C)** The intracellular fluorescence image of **RH-BZN** in complex with Fe^{3+} at 1, 10 and 20 μM

concentration of **RH-BZN** were shown (40X) by counterstained by DAPI and **(D)** by DAPI as nuclear counter stain and LysoTracker for cytoplasm (100X). The lowest concentration of **RH-BZN** (1μm) shows excellent detection of Fe^{3+} in the cytoplasm of HepG2 cell.

ring (**Fig. 4**). The quantum yield of the **RH-BZN–** Fe^{3+} complex was determined to be Φ = 0.57 (with rhodamine 6G as a standard), whereas the free ligand is non- or very weakly fluorescent. The limit of detection (LOD) of Fe^{3+} was determined by the 3σ method and found to be as low as 0.11 μM (**Fig. S12**). All these findings indicate that **RH-BZN** is a good example of an ideal chemosensor for Fe^{3+}.

The formation of the **RH-BZN–** Fe^{3+} complex by opening of the spirolactum ring was established through IR studies. The IR study revealed that the characteristic stretching frequency of the amidic "C=O" of the rhodamine moiety at 1692.15 cm^{-1} is shifted to a lower wave number 1637.68 cm^{-1} in the presence of 1.2 equiv. of Fe^{3+} (**Fig. S3**). This large shift signifies a strong polarization of the C=O bond upon efficient binding to the Fe^{3+} ion and in fact indicates opening of the spirolactum ring.

Bio-imaging of Fe^{3+} by **RH-BZN** was performed in live cell (**Fig. 4 and 5**) by fluorescence microscopic techniques. To determine whether **RH–BZN** has any cytotoxic effect, MMT assay was performed on HepG2 cells which showed no significant cell cytotoxicity up to 80 μm (<30 % cytotoxicity) (**Fig. S6**).[23] Hence further experiments were carried out at low dose (10 μm) of **RH-BZN**.

The intracellular imaging behaviour of **RH-BZN (**10 μM) on HepG2 cells displayed no obvious fluorescence (**Fig. 4**). However, an excellent intracellular cytoplasmic fluorescence was observed inside the cells, when HepG2 cells were incubated with 10 μM **RH-BZN** followed by washing with 1X PBS and subsequent incubation with 10 μM Fe^{3+} and, also subsequent quenching of red fluorescence on treatment with tetra-*n*-butyl ammonium fluoride. Interestingly we have observed that the fluorophore **RH-BZN** shows the only cytoplasmic binding with Fe^{3+}, not the nuclear binding ((**Fig. 4**, inset and **5**). The specific binding of fluorophore **3** into the cytoplasm make this fluorophore less toxic, as fluorophore **3** cannot cross the nuclear membrane to bind to the nucleus (DNA) which cause the more toxic effect to cells.[24] The cytotoxicity study by MMT assay shows 82% cell viability at 20 μM concentration and specifically detects the cytoplasmic Fe^{3+}. Additionally, **Fig. 5** displays the concentration dependent bind ing of **RH-BZN** with intracellular Fe^{3+} which clearly indicates that the present probe is capable of recognizing cytoplasmic Fe^{3+} as low as 1 μm concentration.

As the dye is not water soluble, we performed all the extracellular experiments in MeCN:H_2O (7:3, v/v) mixture. However, when the probe is once solubilised in DMSO it did not give any precipitate on adding water up to 99%. So there was no problem in performing the cell imaging experiment in 1:9 DMSO:H_2O mixture.

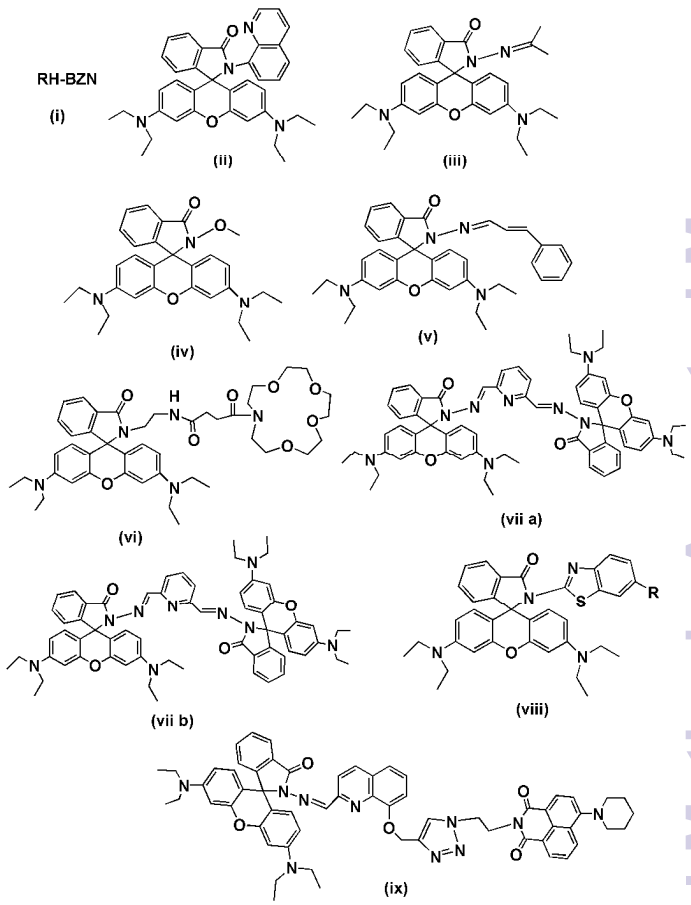

Scheme II

Few of the recently investigated Rhodamine-B based Fe^{3+} sensors are given in **Scheme 2** and some salient features are given in **Table 2**. A quick inspection of these studies reveal that all these are turn on Fe^{3+} ion sensor with moderate LOD values (0.32-5.0 μM) and formation constants (K_f = 5.1 x 10^3 – 4.52 x 10^5 M^{-1}) and applicable for monitoring intracellular Fe^{3+} ion,[25] though in few cases no cell imaging experiments were performed. **RH-BZN** recognizes Fe^{3+} with 240 fold fluorescence enhancement with binding constant of 1.50 x 10^4 M^{-1} and LOD 0.11 μM through 1:1 host-guest type interaction. Not only that the cytoplasmic binding makes this

probe more appropriate for *in vivo* monitoring of Fe^{3+} without any genetic damage.

Table 2. Comparative results of selected rhodamine 6G based probes for recognizing Fe^{3+}.

Probe	Formation constant (M^{-1})	LOD (μM)	Cell
(i) RH-BZN	1.5×10^4	0.11	Done, cytoplasmic binding
(ii)	Not-determined	0.32	Done
(iii)	2.3×10^4	Not determined	Done
(iv)	1.58×10^5	Not determined	Not Done
(v)	Not determined	1.8	Not Done
(vi)	2.46×10^4	0.40	Done
(vii)(a)	7.5×10^3	Not determined	Not done
(vii)(a)	5.1×10^3	Not determined	Not done
(viii)	4.52×10^5	5	Done
(ix)	9.62×10^5	0.05	Done

Conclusions

In summary, a novel *benzoxazine* based dual sensor '*rhodamine-3,4-Dihydro-2H-1,3-benzoxazine*', **RH-BZN** (**3**) has been synthesized and structurally characterized. In 3:7 water:MeCN (v/v) and at physiological pH 7.2, it selectively recognizes Fe^{3+} giving 240 fold fluorescence enhancement and binding constant of 1.50×10^4 M^{-1} through 1:1 host-guest type interaction, which could suitably be employed for cytoplasmic intracellular imaging of Fe^{3+} without notable cytotoxicity. Reversible binding of Fe^{3+} towards this probe was confirmed by reacting with tetra-*n*-butyl ammonium fluoride both in extra- and intra-cellular conditions.

Acknowledgement. Financial support from DST (Ref. SR/S1/IC-20/2012), New Delhi, is gratefully acknowledged.

Notes and references

[a]Department of Chemistry, Jadavpur University, Kolkata 700 032, India, Fax: 91-33-2414-6223, E-mail: **m_ali2062@yahoo.com and *mali@chemistry.jdvu.ac.in***

[b]Molecular & Human Genetics Division , CSIR-Indian Institute of Chemical Biology , 4 Raja S.C. Mallick Road, Kolkata-700032, India

[c] *Department of Chemistry,* Gurudas College, Narkeldanga, Kolkata 700 043, India

Supporting Information Available: Electronic Supplementary Information (ESI) available: X-ray crystallographic files in CIF format and experimental details regarding the synthesis and characterisation of the ligand and metal complex, including spectroscopic details. CCDC No. 1029259. For ESI and crystallographic data in CIF or other electronic format see DOI: 10.1039/c000000x/

References

1. (a) M. Zhang, M. X. Yu, F. Y. Li, M. Zhu, M. Y. Li, Y. Gao, Z. Liu, J. Zhang, D. Zhang, T. Yi and C. H. Huang, *J. Am. Chem. Soc.,* 2007, **129**, 10322; (b) J. H. Lee, C. S. Lim, Y. S. Tian, J. H. Han and B. R. Cho, J. Am. Chem. Soc., 2010, **132**, 1216; (c) Y. Wei, Y. Zhang, Z. Liu and M. L. Guo, *Chem. Commun*., 2010, **46**, 4472.
2. (a) Y. Zhou, F. Wang, Y. Kim, S.-J. Kim and J. Yoon, *Org. Lett.,* 2009, **11**, 4442; (b) B. A. Smith, W. J. Akers, W. M. Leevy, A. J. Lampkins, S. Xiao, W. Wolter, M. A. Suckow, S. Achilefu and B. D. Smith, *J. Am. Chem. Soc.*, 2010, **132**, 67; (c) H. S. Jung, P. S. Kwon, J. W. Lee, J. Kim, C. S. Hong, J. W. Kim, S. Yan, J. Y. Lee, J. H. Lee, T. Joo and J. S. Kim, *J. Am. Chem. Soc.,* 2009, **131**, 2008; (d) L. Huang, X. Wang, G. X. P. Xi, Z. Li, M. Xu, Y. J. Wu, D. C. Bai and Z. Z. Zeng, *Dalton Trans.*, 2010, **39**, 7894; (e) R. Bhowmick, R. Alam, T. Mistri, D. Bhattacharya, P. Karmakar and M. Ali, *Appl. Mater. Inter*., 2015, **7**, 7476; (f) H. Y. Lee, K. M. K. Swamy, J. Y. Jung, G. Kim and J. Yoon, *Sens. Actuators, B* 2013, **182**, 530; (g) F. Wang, S. W. Nam, Z. Guo , S. Park, and J. Yoon, *Sens. Actuators, B* 2012, **161**, 948; (h) X. Chen, T. Pradhan, F. Wang, J. S. Kim and J. Yoon, *Chem. Rev.* 2012, **112**, 1910 (i) P. Mahato, S. Saha, P. Das, H. Agarwalla and A. Das, *RSC Adv.*, 2014,**4**, 36140.
3. (a) S. Bae and J. Tae, *Tetrahedron Lett*., 2007, **48**, 5389; (b) Y. Xiang and A. Tong, *Org. Lett.,* 2006, **8**, 1549; (c) J. L. Bricks, A. Kovalchuk, C. Trieflinger, M. Nofz, M. Buschel, A. I. Tolmachev, J. Daub and K. Rurack, *J. Am. Chem. Soc.*, 2005, **127**, 13522; (d) M. Zhang, Y. Gao, M. Li, M. Yu, F. Li, L. Li, M. Zhu, J. Zhang, T. Yi and C. Huang, *Tetrahedron Lett.,* 2007, **48**, 3709; (e) Y. Liu, Z. Xu, J. Wang, D. Zhang, Y. Yea, and Y. Zhaoa, *Luminescence* 2014; (f) L. Zhang J. Wang, J. Fan, K. Guo, X. Peng, *Bioorg. Med. Chem. Letters*, 2011, **21**, 5413; (g) J. Huang, Y. Xu and X. Qian, *Dalton Trans*., 2014, **43**, 5983.
4. M. Ghaedi, A. Shokrollahi, R. Mehrnoosh, O. Hossaini and M. Soylak, *Cent. Eur. J. Chem.,* 2008, **6**, 488.
5. S. Bae and J. Tae, *Tetrahedron Lett.,* 2007, **48**, 5389.
6. (a) R. Williams, *Pure Appl. Chem.,* 1983, **55**(**1**), 35; (b) M. Ferrali, D. Donati, S. Bambagioni, M. Fontani, G. Giorgic and A. Pietrangelod, *Bioorg. Med. Chem.,* 2001, **9**, 3041.
7. P. Aisen, M. Resnick and E. Leibold, *Curr.Opin. Chem. Biol.,* 1999, **3**, 200.
8. D. Touati, *Arch. Biochem. Biophys*., 2000, **373**, 1.

9. (a) J. R. Burdo and J. R. Connor, *Biometals,* 2003, **16**, 63; (b) J. R. Connor, S. L. Menzies, S. M. St. Martin and E. J. Mufson, *J. Neurosci. Res.,* 1990, **27**, 595; (c) R. R. Crichton, S. Wilmet, R. Legssyer and R. J. Ward, *J. Inorg. Biochem.,* 2002, **91**, 9; (d) R. S. Eisenstein, *Annu. Rev. Nutr.,* 2000, **20**, 627.
10. (a) B. T. Felt and B. Lozoff, *J. Nutr.,* 1996, **126**, 693; (b) C. J. Earley, J. R. Connor, J. L. Beard, E. A. Malecki, D. K. Epstein and R. P. Allen, *Neurology*, 2000, **54**, 1698.
11. (a) J. P. Sumner and R. Kopelman, *Analyst*, 2005, **130**, 528;(b) Y. Ma, W. Luo, P. J. Quinn, Z. Liu and R. C. Hider, *J. Med. Chem*., 2004, **47**, 6349; (c) G. E. Tumambac, C. M. Rosencrance and C. Wolf, *Tetrahedron*, 2004, **60**, 11293; (d) A. Ali, Q. Zhang, J. Dai and X. Huang, *BioMetals*, 2003, **16**, 285.
12. (a) J. Mao, L. Wang, W. Dou, X. Tang, Y. Yan and W. Liu, *Org. Lett.,* 2007, **9**, 4567; (b) M. Xu, S. Wu, F. Zeng and C. Yu, *Langmuir*, 2010, **26**, 4529; (c) X. Wu, B. Xu, H. Tong and L. Wang, *Macromolecules*, 2010, **43**, 8917.
13. T. Besson, C. W. Rees, G. Cottenceau and A. Pons.*Bioorg. Med. Chem. Lett*., 1996, **6**, 2343.
14. S. Ozden, A. Ozturk, H. Goker and N. Altanlar, *I. L. Farma*, 2000, **55**, 715.
15. R. Fringuelli, D. Pietrella, F. Schiaffella, A. Guarraci, S. Perito, F. Bistoni and A.Vecchiarilli, *Bioorg. Med. Chem.,* 2002, **10**, 1681.
16. S. Alper-Hayta, E. Aki-Sener, B. Tekiner-Gulbas, I. Yildiz, I. Yalcin and N. Alanlar. *Eur. J. Med. Chem*., 2006, **41**, 1398.
17. B. P. Mathew, A. Kumar, S. Sharma, P.K. Shukla and M. Nath. *Eur. J. Med. Chem.,* 2010, **45**, 1502.
18. K. Waisser, J Gregor, L. Kubicova, V. Klimesova, J. Kunes, M. Machacek and J. Kaustova, *Eur. J. Med. Chem*., 2000, **35**, 733.
19. P. Hsieh, F. Chong, C. Chang, F. Zheng and K. H. Lin. *Bioorg. Med. Chem. Lett.*, 2004, **14**, 4751.
20. K. M. Pritchard, J. A. Rawi; C. Bradley*, Eur. J. Med. Chem.,* 2007, **42**, 1200.
21. C. R. Lohani, J. M. Kim, S. Y. Chung, J. Yoon and K. H. Lee, *Analyst*, 2010, **135**, 2079.
22. T. Mistri, R. Alam, M. Dolai, S. K. Mandal, P. Guha, A. R. KhudaBukhsh and M. Ali, *Eur. J. Inorg. Chem.* 2013, 585.
23. R. Bhowmick, M. Dolai, R. Alam, T. Mistri, A. Katarkar, K. Chaudhuri and M. Ali, *RSC Adv.*, 2014, **4**, 41784.
24. F. Di Maria, I. E. Palamà, M. Baroncini, A. Barbieri, A. Bongini, R. Bizzarri, G. Gigli and G. Barbarella, *Org. Biomol. Chem.,* 2014, **12**, 1603.
25. (a) J. Huang, Y. Xua and X. Qia, *Dalton Trans*., 2014, **43**, 5983; (b) M. Zhang, Y. Gao, M. Li, M. Yu, F. Li, L. Li, M. Zhu, J. Zhang, T. Yia and C. Huang, *Tetrahedron Letters,* 2007, **48**, 3709; (c) S. Bae and J. Tae, *Tetrahedron Letters,* 2007, **48**, 5389; (d) Y. Liu, Z. Xu, J. Wang, D. Zhang, Y. Yea and Y. Zhaoa, *Luminescence,* 2014, **29,** 945; (e) X. Baoa, X. Caoa, X. Niec, Y. Xub, W. Guod, B. Zhouc, L. Zhangb, H. Liaob and T. Pang, *Sensors and Actuators B*, 2015, **208**, 54; (f) A. J. Weerasinghe, C. Schmiesing, S. Varaganti, G. Ramakrishna,* and E. Sinn, *J. Phys. Chem. B,* 2010, **114**, 9413; (g) Z. Yang, M. She, B. Yin, J. Cui, Y. Zhang, W. Sun, J. Li and Z. Shi, *J. Org. Chem.*, 2012, **77**, 1143;(h) N. R. Chereddy, S. Thennarasu and A. B. Mandal, *Analyst*, 2013, **138**,1334.

Journal Name

RSCPublishing

Article

A novel *rhodamine-3,4-dihydro-2H-1,3-benzoxazine* conjugate as a highly sensitive and selective chemosensor for Fe^{3+} ion with cytoplasmic cell imaging possibilities

Habib Ali Molla[a], Rahul Bhowmick[a], Atul Katarkar[b], Keya Chaudhuri[b], Sumana Gangopadhyay[c], and Mahammad Ali[a]**

A novel *rhodamine-3,4-dihydro-2H-1,3-benzoxazine* conjugate exhibits excellent selectivity towards Fe^{3+} both in extra and intracellular conditions.